catalysts

MDPI

Article

Facile Construction of Magnetic Ionic Liquid Supported Silica for Aerobic Oxidative Desulfurization in Fuel

Fujie Liu [1], Ming Zhang [2,*], Yongkang Gao [2], Haojie Tan [2], Hongping Li [2], Chao Wang [3], Wenshuai Zhu [2,*] and Huaming Li [2]

[1] Zhenjiang Key Laboratory of Functional Chemistry, Institute of Medicine and Chemical Engineering, Zhenjiang College, Zhenjiang 212028, China; fjie520@163.com
[2] Institute for Energy Research, School of Chemistry and Chemical Engineering, Jiangsu University, Zhenjiang 212013, China; gaoyongkang1997@163.com (Y.G.); haojietan2021@163.com (H.T.); hongpingli@ujs.edu.cn (H.L.); lhm@ujs.edu.cn (H.L.)
[3] Jingjiang College, Jiangsu University, Zhenjiang 212114, China; chaowang@ujs.edu.cn
* Correspondence: zm@ujs.edu.cn (M.Z.); zhuws@ujs.edu.cn (W.Z.); Tel.: +86-511-88799500 (W.Z.); Fax: +86-511-88791708 (W.Z.)

Abstract: With the rapid growth in fuel demand, deep desulfurization of fuel oil is vitally necessary for the sake of health and environmental protection. In this work, a kind of magnetic ionic liquid supported silica is prepared by a facile ball milling method, and applied in the aerobic oxidative desulfurization of organosulfurs in fuel. The experimental results indicated that ball milling procedure can increase the specific surface area of samples, which is beneficial to oxidative desulfurization process. Under the optimal reaction conditions, the prepared materials can have an entire removal of aromatic sulfur compounds as well as a good recycling ability. Moreover, the introduction of Fe_3O_4 did not decline the desulfurization performance, but help the catalyst to be easily separated after reaction.

Keywords: polyoxometalate; ionic liquid; silica; magnetic materials; ball milling

Citation: Liu, F.; Zhang, M.; Gao, Y.; Tan, H.; Li, H.; Wang, C.; Zhu, W.; Li, H. Facile Construction of Magnetic Ionic Liquid Supported Silica for Aerobic Oxidative Desulfurization in Fuel. *Catalysts* **2021**, *11*, 1496. https://doi.org/10.3390/catal11121496

Academic Editor: Haralampos N. Miras

Received: 8 October 2021
Accepted: 30 November 2021
Published: 9 December 2021

1. Introduction

With the rapid development of the automobile industry, the demand for fuel oil was greatly increased in the past decades. However, sulfur compounds in fuel oil are converted to SO_X after combustion, which is a major source of acid rain, haze, and air pollution [1–4]. Hence, the legal threshold values for sulfur content in fuel oil is limited to less than 10 ppm in many countries [5–7]. Currently, the traditional technology to remove sulfur compounds in the oil refining industry is hydrodesulfurization (HDS), which is extremely efficient in removing aliphatic and acrylic sulfur compounding such as thiols, sulfides, and disulfides. However, it is difficult to apply in the removal of aromatic sulfur compounds such as dibenzothiophene (DBT) and its derivatives [8,9]. Hence, some supplementary technologies have been developed, including extraction desulfurization (EDS), adsorption desulfurization (ADS), biological desulfurization (BDS), and oxidative desulfurization (ODS) [10–14]. In particular, ODS is considered to be a promising technology, which can efficiently remove aromatic sulfur compounds under mild conditions. Therefore, deep oxidative desulfurization is a very important research topic, especially using green oxidants such as molecular oxygen.

The choice of catalyst is also critical for the ODS process. Various kinds of materials have been applied in the ODS process, including organic acids, inorganic acids, and peroxide materials [15]. Although these homogeneous catalysts exhibit high activity, it is difficult for them to be separated from the ODS system after reaction. In order to solve this problem, a series of heterogeneous catalysts have gradually been developed [16–18], such as metal oxides [19–21], activated carbon [22], molecular sieves (e.g., SBA-15 and MCM-41) [23,24], and polyoxometalates (POMs) [25–27]. Among them, polyoxometalate (POMs)

catalysts have attracted wide attention for their advantages of strong redox properties, environmental friendliness, and high designability. However, due to the high lattice energy, most POMs materials have poor dispersibility in organic solvents, resulting in low activity in ODS process [26,27]. To solve this problem, Li's group [25,28,29] designed a series of ionic liquids (ILs) with organic cation and POMs-based anion to improve the interface between the catalyst and oil phase, promoting the desulfurization performance. However, the low specific surface area of POMs materials often leads to a long reaction time and poor recycling performance. Hence, the immobilization of POMs onto suitable carriers would solve the problem of improving the catalytic activity in oxidative desulfurization [30–36]. Hence, various types of POMs supported materials such as W-SiO_2-type [12,13,37–39], Mo-SiO_2-type [40–42], V-SiO_2-type [43], and Au-SiO_2-type [44,45] have been studied, exhibiting good activity in the ODS process. However, the used catalysts could not be easily separated from the recycling system, and other separation methods such as centrifugation are required, increasing the energy consumption and reaction cost. Magnetic nanocomposites such as Fe_3O_4 are a type of material that can be moved by an external magnetic field [46]. Therefore, Fe_3O_4 has the application potential for rapid separation of the catalyst after the desulfurization reaction. On the other hand, mechanochemical methods have been widely explored in the preparation of catalysts due to their advantages such as being solvent-free, environmentally friendly, and their rapid preparation [47–49].

In this work, a kind of magnetic ionic liquid supported silica ($C_{16}PW/SiO_2$-Fe-BM) is prepared by a facile ball milling method, and applied in the aerobic oxidative desulfurization of organosulfurs in fuel. The physicochemical properties of the catalyst were characterized by various technical methods such as FT-IR, Raman, BET, and XPS. The catalytic performance of the catalyst was evaluated by oxidizing the sulfides in the presence of oxygen. The effect of Fe_3O_4 on the magnetic properties was also investigated as well as the desulfurization performance. The experimental results demonstrated that the sample $C_{16}PW/SiO_2$-Fe-BM exhibited good desulfurization activity, which can be quickly separated after reaction.

2. Results and Discussion

2.1. Characterization of Samples

FT-IR spectra of various samples is depicted in Figure 1. For the ionic liquid $C_{16}PW$, four characteristic peaks of Keggin structure could be observed in the region of 800–1100 nm^{-1} (Figure 1a), which was assigned to the vibration band of P–O (1080 cm^{-1}), W=O (982 cm^{-1}), W–O_c–W (corner-sharing, 897 cm^{-1}) and W–O_e–W (edge-sharing, 806 cm^{-1}), respectively [50]. For IL supported silica catalysts (Figure 1b–d), the main vibration peaks for Keggin units could also be found as well as the symmetrical stretching vibration of Si–O–Si (800 cm^{-1}) and tetrahedron bending vibration of [SiO_4] (469 cm^{-1}) [51]. In addition, C–H stretching vibration peaks of ionic liquid cations appeared in the range of 2800 to 2900 cm^{-1}. These results indicated that the ionic liquid $[C_{16}mim]_3PW_{12}O_{40}$ was successfully introduced to the SiO_2.

Figure 2 shows the Raman spectra of various samples. For $C_{16}PW$ (Figure 2a), two distinct peaks at 1006 and 991 cm^{-1} could be observed, which was respectively ascribed to ν_s(W=O) and ν_{as}(W=O) in the Keggin units [52]. After introduction to silica (Figure 2b–d), the two peaks were red-shifted in the Raman spectra, which may be due to the reduced interaction between the bonds of W=O. No obvious bands for Fe_3O_4 was observed in the Raman spectra, which could be attributed to the low Raman intensity of Fe_3O_4 with a low content. These results also indicated that ionic liquid was successfully supported, and retained its structure.

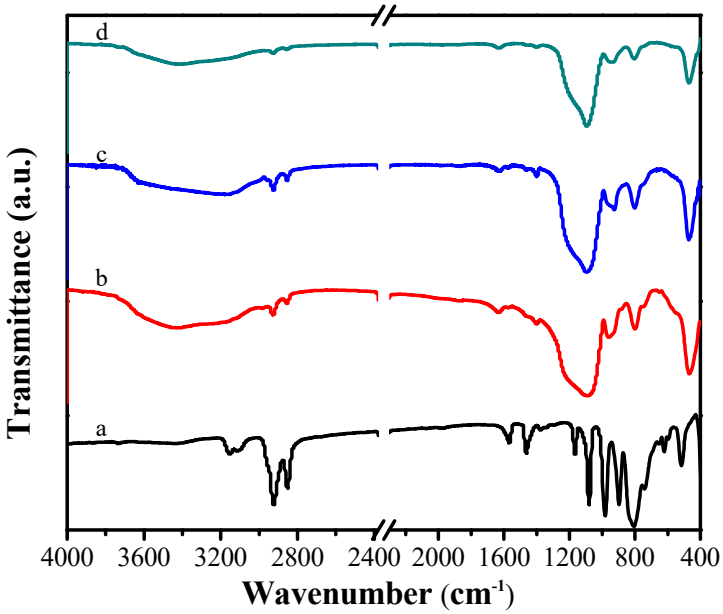

Figure 1. FT-IR spectra of various samples. (**a**) $C_{16}PW$, (**b**) $C_{16}PW/SiO_2$, (**c**) $C_{16}PW/SiO_2$-BM, (**d**) $C_{16}PW/SiO_2$-Fe-BM.

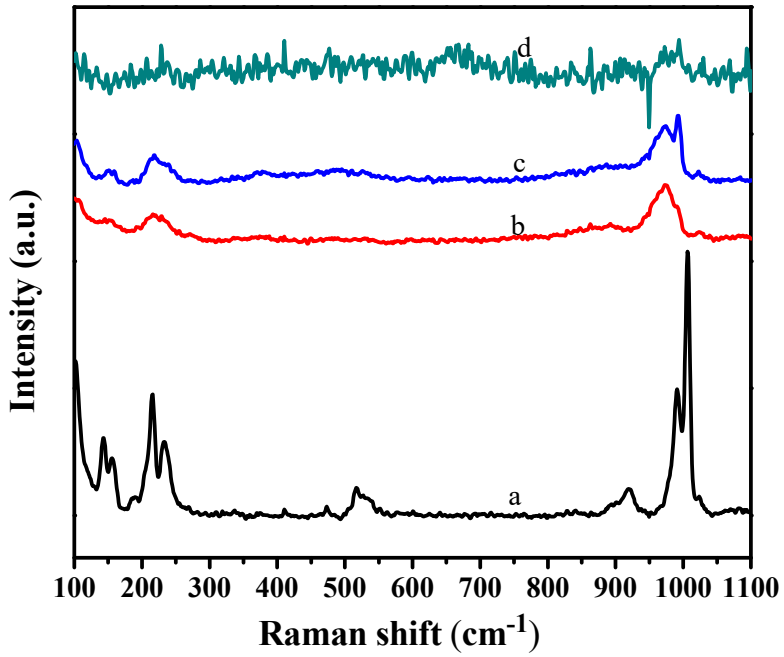

Figure 2. Raman spectra of various samples. (**a**) $C_{16}PW$, (**b**) $C_{16}PW/SiO_2$, (**c**) $C_{16}PW/SiO_2$-BM, (**d**) $C_{16}PW/SiO_2$-Fe-BM.

Ultraviolet-visible diffuse reflectance spectroscopy is performed to investigate the electron transfer in different samples (Figure 3). For the ionic liquid $C_{16}PW$ (Figure 3a), the absorption peaks could be observed around 268 and 208 nm assigned to the charge transfer of $O^{2-} \rightarrow W^{6+}$ and O→P [53]. For the ionic liquid supported materials, the broad and strong absorption peaks could be found in the range 200–400 nm, which may be due to the charge transfer induced by the excitation electron from the valence band to the conduction band [54]. The results also indicated the successful synthesis of the ionic liquids supported materials.

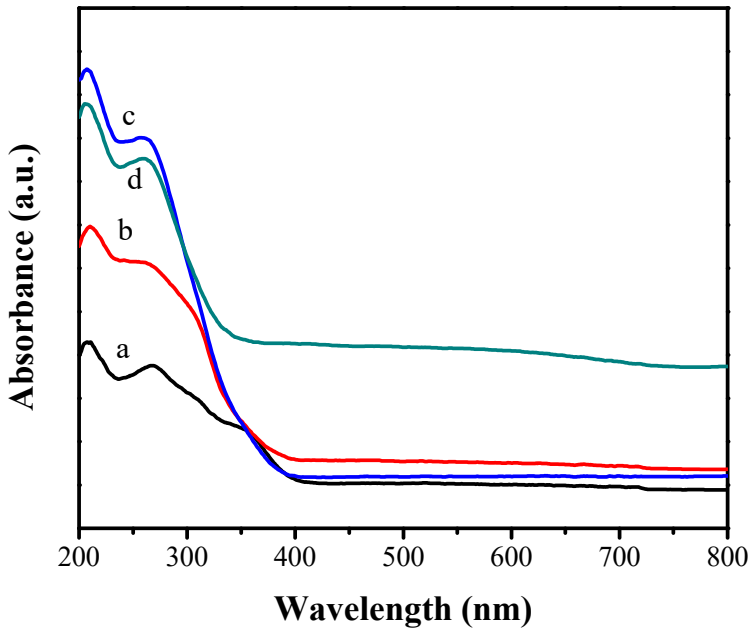

Figure 3. UV-vis DRS spectra of various samples. (**a**) $C_{16}PW$, (**b**) $C_{16}PW/SiO_2$, (**c**) $C_{16}PW/SiO_2$-BM, (**d**) $C_{16}PW/SiO_2$-Fe-BM.

XPS spectra are employed to investigate the effect of ball milling method and Fe_3O_4 incorporation on the chemical properties on the elements of various samples (Figure 4). For the W 4f core-level spectrum of $C_{16}PW/SiO_2$ (Figure 4a), two peaks at the binding energy of 37.38 eV and 35.23 eV could be found, which was ascribed to W $4f_{5/2}$ and W $4f_{7/2}$ respectively. For the sample $C_{16}PW/SiO_2$-BM, the peak for the W $4f_{5/2}$ and W $4f_{7/2}$ could be observed at the same position (Figure 4b), indicating no change on the valence state of tungsten after ball milling. However, for the sample $C_{16}PW/SiO_2$-Fe-BM (Figure 4c), the binding energy for W $4f_{5/2}$ and W $4f_{7/2}$ was increased to 38.18 eV and 36.03 eV, indicating the electron transfer between Fe_3O_4 and supported ionic liquid.

N_2 adsorption–desorption isotherms of various samples are presented to study the porous property (Figure 5). According to the classification of the IUPAC, all the samples exhibited a typical type-IV curve [55]. For the sample $C_{16}PW/SiO_2$ (Figure 5a), a H3 hysteresis loop appeared in $0.55 < p/p_o < 0.95$, indicating the presence of a stacking hole in the catalyst. For $C_{16}PW/SiO_2$-BM and $C_{16}PW/SiO_2$-Fe-BM (Figure 5b,c), a H2 hysteresis loop could be found in the relative pressure of 0.45–1.0, indicating the slit pores existing in the samples. These results demonstrated that the ball milling method could reduce the particle size and increase the specific surface area (Table 1). Moreover, the incorporation of Fe_3O_4 during the grinding process could further increase the specific surface area, which is beneficial for the ODS process.

Table 1. The porous properties of various samples.

Entry	Sample	S_{BET} (m^2/g)	Pore Diameter (nm)	Pore Volume (nm)
1	$C_{16}PW/SiO_2$	28.8	4.5	0.11
2	$C_{16}PW/SiO_2$-BM	76.7	8.4	0.16
3	$C_{16}PW/SiO_2$-Fe-BM	107.8	7.8	0.21

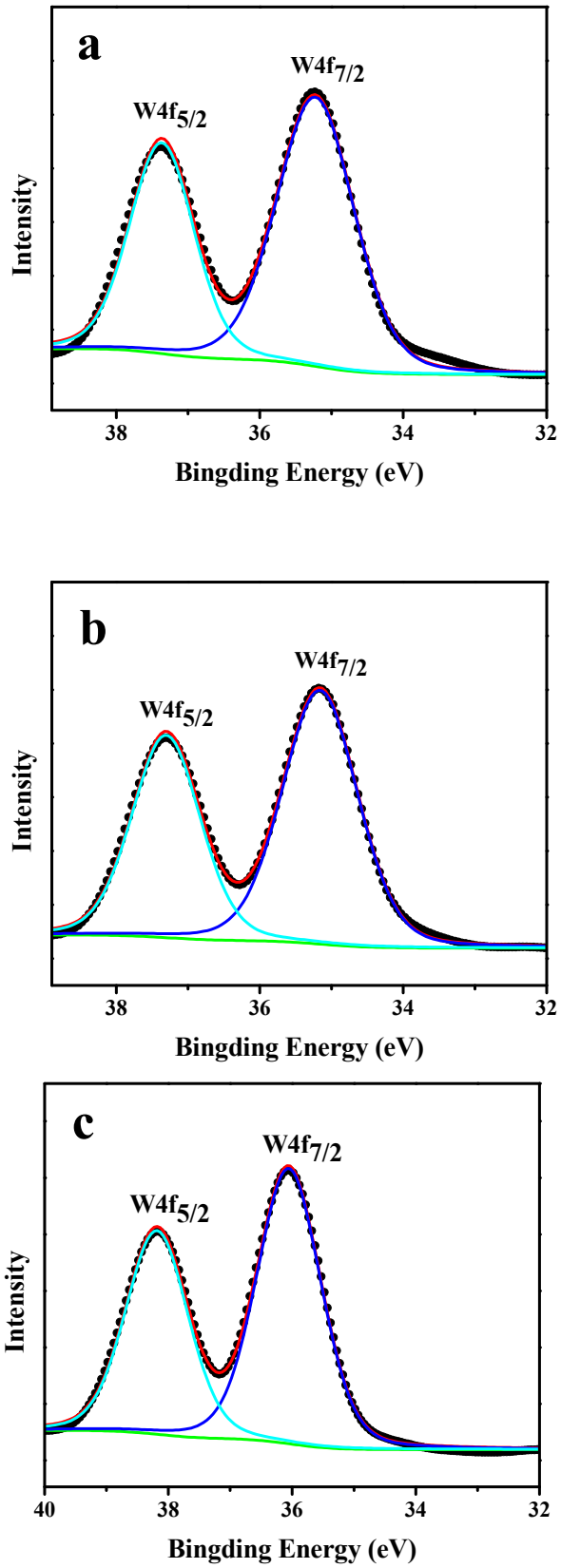

Figure 4. XPS survey spectra of (**a**) $C_{16}PW/SiO_2$; (**b**) $C_{16}PW/SiO_2$-BM; (**c**) $C_{16}PW/SiO_2$-Fe-BM.

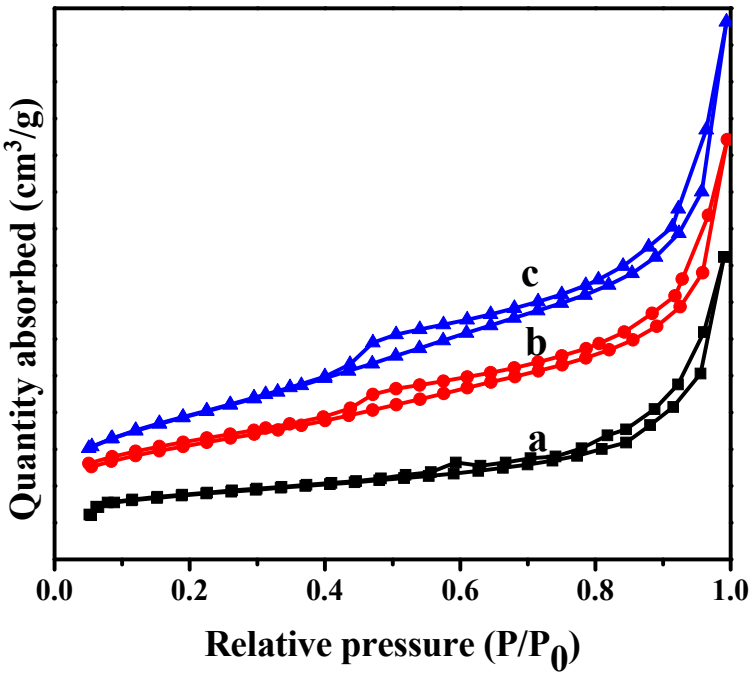

Figure 5. N_2 adsorption–desorption isotherms of various samples. (**a**) $C_{16}PW/SiO_2$; (**b**) $C_{16}PW/SiO_2$-BM; (**c**) $C_{16}PW/SiO_2$-Fe-BM.

2.2. ODS Performance

The desulfurization performance of different samples is presented in Figure 6. Under the same reaction conditions, the sulfur removal for $C_{16}PW/SiO_2$, $C_{16}PW/SiO_2$-BM, and $C_{16}PW/SiO_2$-Fe-BM could reach 24.9%, 98.5%, and 99.1%, respectively. It could be found that the ODS performance of the samples was improved after ball milling. Moreover, the desulfurization efficiency was also increased after the incorporation of Fe_3O_4, which was ascribed to the higher surface area (Table 1).

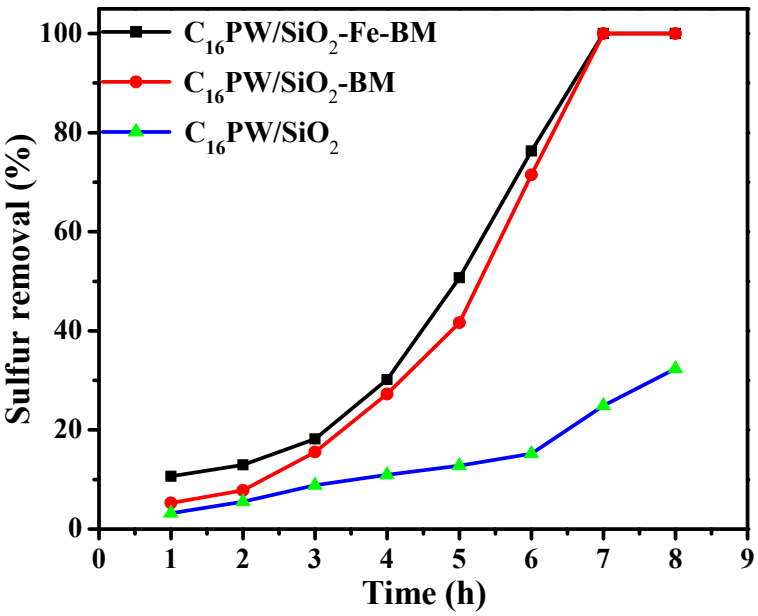

Figure 6. ODS performance of various samples. Experimental conditions: T = 120 °C, m (catalyst) = 0.05 g, air flow:100 mL/min.

In order to study the desulfurization activity of the sample $C_{16}PW/SiO_2$-Fe-BM toward different sulfur-containing substrates, the typical sulfide DBT and its derivatives (4-MDBT and 4,6-DMDBT) are carried out under the same conditions (Figure 7). For DBT, the desulfurization rate can reach 100% within 7 h. On the other hand, the desulfurization rate toward the aromatic sulfide 4-MDBT and 4,6-DMDBT can reach 90.2% and 80.5% in 8 h, respectively. The difference on ODS performance may be ascribed to the steric hindrance in the sulfur compounds [56]. The steric hindrance of sulfur compounds followed the order: 4,6-DMDBT > 4-MDBT > DBT [57]. Compared to DBT, 4-MDBT and 4,6-DMDBT have one or two more methyl groups on the benzene ring, respectively. Their steric hindrance is greater than that of DBT, making it difficult for sulfur atoms to be oxidized during the reaction process.

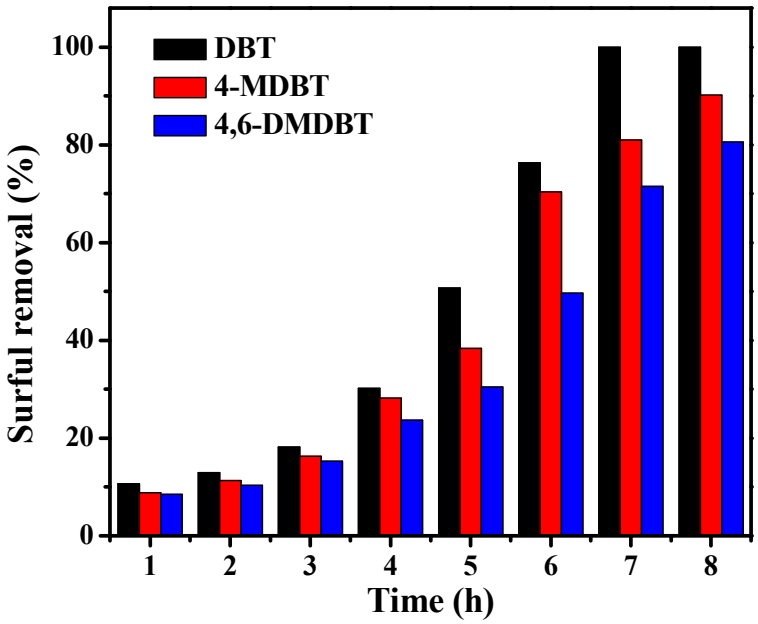

Figure 7. ODS performance of different sulfur-containing substrates in the desulfurization system.Experimental conditions: T = 120 °C, m(Catalyst) = 0.05 g, air flow: 100 mL/min.

The recycling performance of the catalyst is another important factor in the desulfurization process (Figure 8). The recycling process of the typical sample $C_{16}PW/SiO_2$-Fe-BM was performed as follows: The upper oil phase was decanted directly after the reaction, and the lower catalyst was dried at 50 °C overnight. Afterwards, the next run was evaluated after adding the fresh model oil and air flow. It can be observed that the sulfur removal could still reach 100% after being recycled four times.

2.3. Magnetic Hysteresis Test

In order to investigate the magnetism of the catalyst, the magnetization of Fe_3O_4 and $C_{16}PW/SiO_2$-Fe-BM is measured through an external magnetic field at room temperature (Figure 9). As shown in Figure 9A,B, the saturation magnetization of $C_{16}PW/SiO_2$-Fe-BM (0.8 emg/g) is significantly lower than that of Fe_3O_4 (82 emg/g). This result was attributed to the low content of Fe_3O_4 and the addition of non-magnetic material ($C_{16}PW/SiO_2$) in the hybrid materials. Moreover, no hysteresis phenomenon was found in Figure 9A, indicating the superparamagnetism of the prepared samples. To further confirm the above results, the separation expriment of the sample in oil is carried out in this study (Figure 9C). It was obviously found that the catalyst could be easily separated from the oil phase through the action of an external magnetic field.

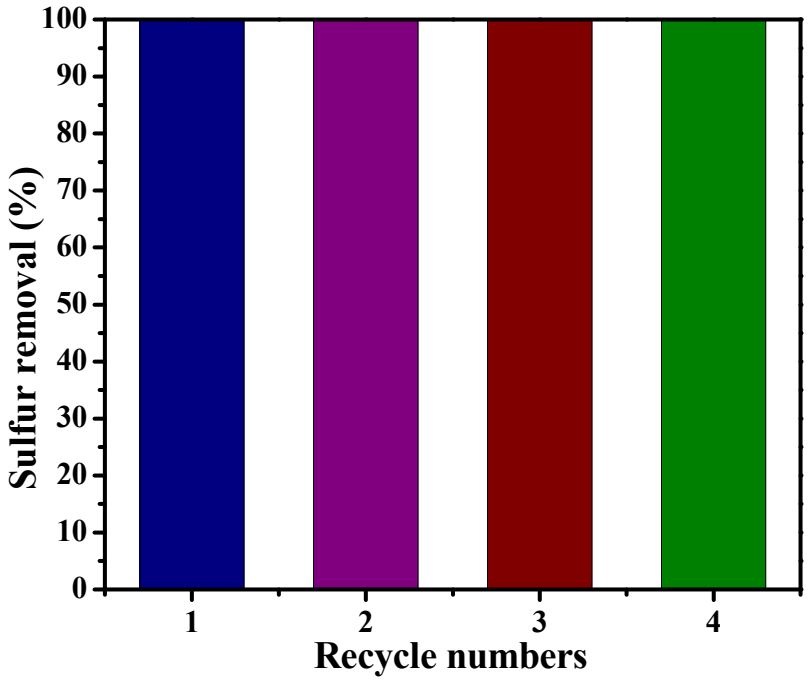

Figure 8. Recycle of the reaction system. Experiment conditions: m(catalyst) = 0.05 g, t = 8 h, T = 120 °C.

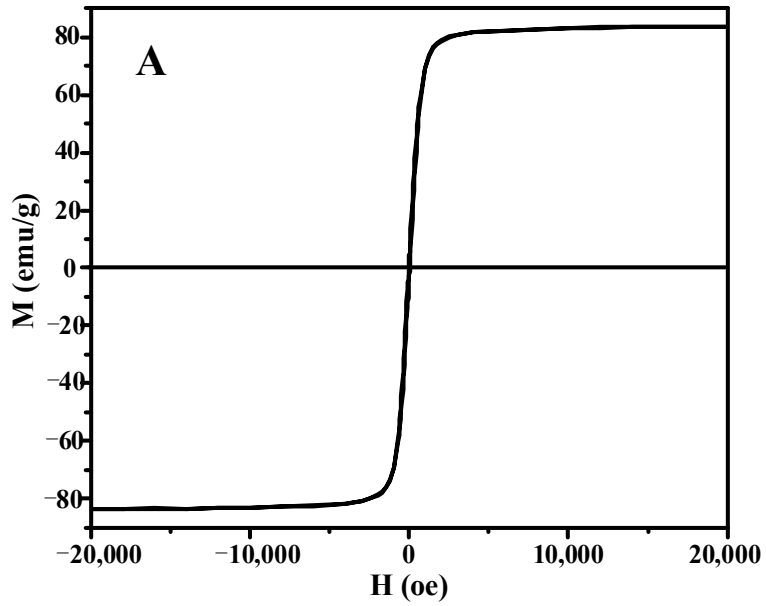

Figure 9. *Cont*.

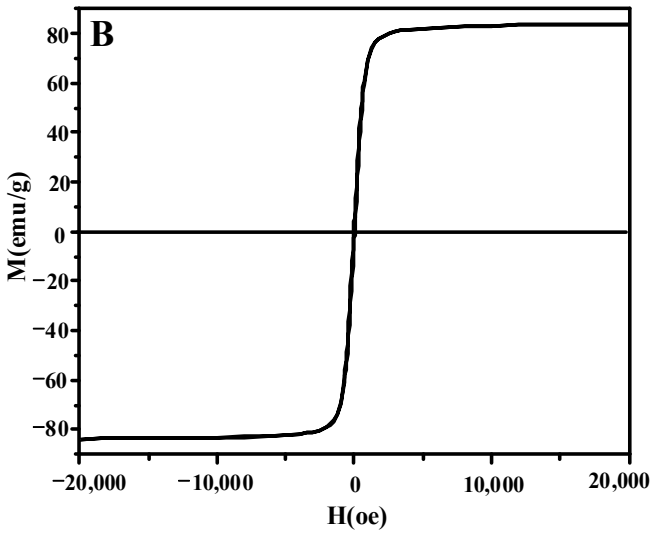

Figure 9. Magnetization curves for Fe_3O_4 (**A**) and $C_{16}PW/SiO_2$-Fe-BM (**B**); Separation of the sample from oil phase using an external magnet (**C**).

3. Experimental Section

3.1. Materials

Phosphotungstic acid (HPW) was obtained from Sigma-Aldrich. 1-Hexadecyl-3-methyl-imidazolium chloride ($[C_{16}mim]Cl$) was purchased from Shanghai Chenjie Chemical Co., Ltd. (Shanghai, China). Acetonitrile (CH_3CN), tetraethyl orthosilicate (TEOS), ammonia ($NH_3 \cdot H_2O$), ferrous chloride hexahydrate ($FeCl_3 \cdot 6H_2O$), Sodium acetate trihydrate ($CH_3COONa \cdot 3H_2O$) were supplied by Sinopharm Chemical Reagents Co., Ltd. (Shanghai, China). Dibenzothiophene (DBT, 98%), 4-methyldibenzothiophene (4-MDBT,96%) and 4,6-dimethyldibenzothiphene (4,6-DMDBT, 97%) were marketed from Shanghai Chemical Reagent Co. Ltd. (Shanghai, China).

3.2. Synthesis of Magnetic Fe_3O_4

A total of 3.0 g $FeCl_3 \cdot 6H_2O$ was dissolved in 60 mL of ethylene glycol with continuous stirring for 30 min. Afterwards, 6.0 g $CH_3COONa \cdot 3H_2O$ was added to the above solution with continuous stirring for 30 min. The mixed solution was transferred to a reaction kettle and kept at 200 °C for 12 h. Finally, the precipitate was collected by a magnet, washed with water and alcohol for several times, and dried at 50 °C in a vacuum.

3.3. Synthesis of Catalysts

Ionic liquid $[C_{16}mim]_3PW_{12}O_{40}$ ($C_{16}PW$) was synthesized according to the previous report [58]. In a typical process, 0.3 g of $C_{16}PW$ was dissolved in 4 mL of acetonitrile with continuous stirring. The above solution was dropwise added to 26 mL of deionized water at 30 °C under stirring for 10 min. Subsequently, 2 mL of TEOS and 0.5 mL of aqueous ammonia was dropwise added to the above mixture. After stirring for 3 h, the resulting solution was dried at 50 °C overnight to obtain the supported ionic liquid $C_{16}PW/SiO_2$. Finally, $C_{16}PW/SiO_2$ was mechanically milled with magnetic Fe_3O_4 (1 wt.%) with a rotation speed of 200 rpm for 3 h to obtain $C_{16}PW/SiO_2$-Fe-BM (Scheme 1). For comparison, supported ionic liquid $C_{16}PW/SiO_2$ without Fe_3O_4 is obtained with the same ball milling method and is denoted as $C_{16}PW/SiO_2$-BM.

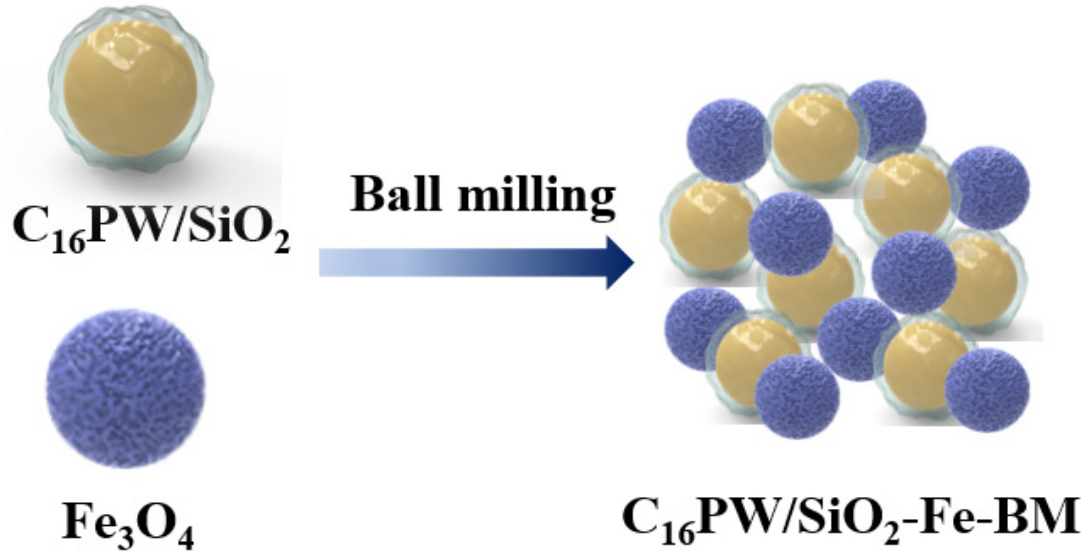

Scheme 1. The preparation process of samples.

3.4. Oxidative Desulfurization Process

The model oil was prepared by dissolving DBT, 4-MDBT, and 4,6-DMDBT in dodecane with a corresponding S-concentration of 200 ppm, respectively. In a typical reaction process, 0.01 g of the prepared samples and 20 mL of model oil was added in a three-necked flask equipped with a magnetic stirrer and a heater set at a certain temperature. Then, the air was injected to the reactor at a flow rate of 100 mL/min. The residual sulfur content in the model oil was determined by gas chromatography on Shimadzu GC 2010 Plus (SH-Rtx-5, 30 m × 0.25 mm × 0.25 μm). The injector temperature was 250 °C, and the detector temperature was 300 °C. The temperature of the GC process started at 100 °C and rose to 250 °C at 25 °C/min.

3.5. Characterization

Fourier transform infrared spectra (FT-IR) of the samples (KBr pellets) were recorded on a Nicolet FT-IR spectrophotometer (Nexus 470, Thermo Electron Corporation, Waltham, MA, USA) with a range of 400–4000 cm^{-1} at room temperature. Crystalline structures of hybrid materials were analyzed by the XRD technique using an X-ray diffractometer (Bruker D8 ADVANCE, Billerica, MA, USA) using Cu Kα radiation at 30 kV (λ = 1.54 Å). The Raman spectrum was obtained on a DXR Raman microscope (Waltham, MA, USA) with a 532 nm laser source under ambient conditions at room temperature. The wavenumbers range from 400 to 4000 cm^{-1}. X-ray photoelectron spectroscopy (XPS) was recorded on a spectrophotometer (Thermo VG, Waltham, MA, United States) with 30 eV energy to explore the scanning of the narrow spectra of the elements on the surface. Textural properties were measured by Nitrogen adsorption–desorption isotherms. It was carried out using

Micromeritics ASAP 2000 equipment (Norcross, GA, USA) at liquid N_2 temperature. The content of sulfur-containing left in oil phase was characterized by Gas chromatography-mass spectrometry (GC-MS7890/5975C-GC/MSD, Agilent, Santa Clara, CA, USA).

4. Conclusions

To sum up, magnetic ionic liquid supported silica ($C_{16}PW/SiO_2$-Fe-BM) was synthesized by ball milling and applied in the removal of organic sulfides with oxygen as the oxidant. The experimental results indicated that polyoxometalate based ionic liquids was successfully introduced to the silica as well as the Fe_3O_4 particle to give the prepared sample superparamagnetism. In the aerobic oxidative desulfurization process, the hybrid catalyst exhibited good catalytic performance, which could achieve complete removal of dibenzothiophene in 7 h. Without any further regeneration procedure, the sulfur removal could still reach 100% after being recycled four times. The desulfurization performance of various aromatic sulfur compounds decreased in the order of DBT > 4-MDBT > 4,6-DMDBT.

Author Contributions: Conceptualization, M.Z. and W.Z.; methodology, Y.G.; software, H.L. (Hongping Li); validation, F.L., M.Z. and W.Z.; formal analysis, H.T.; investigation, C.W.; resources, H.L. (Huaming Li); data curation, F.L.; writing—original draft preparation, F.L.; writing—review and editing, Y.G.; visualization, H.T.; supervision, H.L. (Huaming Li); project administration, M.Z.; funding acquisition, H.L (Huaming Li). All authors have read and agreed to the published version of the manuscript.

Funding: Financial support from the National Natural Science Foundation of China (Nos. 21722604 and 21776116), the Society Development Fund of Zhenjiang City (SH2020020).

Data Availability Statement: The data presented in this study are available in article.

Acknowledgments: Thanks for the financial support from the National Natural Science Foundation of China (Nos. 21722604 and 21776116), the Society Development Fund of Zhenjiang City (SH2020020).

Conflicts of Interest: The authors declare no conflict of interest.

References

1. Bertleff, B.; Claussnitzer, J.; Korth, W.; Wasserscheid, P.; Jess, A.; Albert, J. Extraction coupled oxidative desulfurization of fuels to sulfate and water-soluble sulfur compounds using polyoxometalate catalysts and molecular oxygen. *ACS Sustain. Chem. Eng.* **2017**, *5*, 4110–4118. [CrossRef]
2. Piccinino, D.; Abdalghani, I.; Botta, G.; Crucianelli, M.; Passacantando, M.; Di Vacri, M.L.; Saladino, R. Preparation of wrapped carbon nanotubes poly(4-vinylpyridine)/MTO based heterogeneous catalysts for the oxidative desulfurization (ODS) of model and synthetic diesel fuel. *Appl. Catal. B Environ.* **2017**, *200*, 392–401. [CrossRef]
3. Ganiyu, S.A.; Alhooshani, K.; Ali, S.A. Single-pot synthesis of Ti-SBA-15-NiMo hydrodesulfurization catalysts: Role of calcination temperature on dispersion and activity. *Appl. Catal. B Environ.* **2017**, *203*, 428–441. [CrossRef]
4. Zhu, W.S.; Wang, C.; Li, H.P.; Wu, P.W.; Xun, S.H.; Jiang, W.; Chen, Z.G.; Zhao, Z.; Li, H.M. One-pot extraction combined with metal-free photochemical aerobic oxidative desulfurization in deep eutectic solvent. *Green Chem.* **2015**, *17*, 2464–2472. [CrossRef]
5. Sampanthar, J.T.; Xiao, H.; Dou, H.; Nah, T.Y.; Rong, X.; Kwan, W.P. A novel oxidative desulfurization process to remove refractory sulfur compounds from diesel fuel. *Appl. Catal. B Environ.* **2006**, *63*, 85–93. [CrossRef]
6. Song, C.; Ma, X. New design approaches to ultra-clean diesel fuels by deep desulfurization and deep dearomatization. *Appl. Catal. B Environ.* **2003**, *41*, 207–238. [CrossRef]
7. Al-Shahrani, F.; Xiao, T.C.; Llewellyn, S.A.; Barri, S.; Jiang, Z.; Shi, H.H.; Martinie, G.; Green, M.L.H. Desulfurization of diesel via the H_2O_2 oxidation of aromatic sulfides to sulfones using a tungstate catalyst. *Appl. Catal. B Environ.* **2007**, *73*, 311–316. [CrossRef]
8. Zhang, M.; Zhu, W.; Li, H.; Xun, S.; Ding, W.; Liu, J.; Zhao, Z.; Wang, Q. One-pot synthesis, characterization and desulfurization of functional mesoporous W-MCM-41 from POM-based ionic liquids. *Chem. Eng. J.* **2014**, *243*, 386–393. [CrossRef]
9. Gu, Q.Q.; Zhu, W.S.; Xun, S.H.; Chang, Y.H.; Xiong, J.; Zhang, M.; Jiang, W.; Zhu, F.X.; Li, H.M. Preparation of highly dispersed tungsten species within mesoporous silica by ionic liquid and their enhanced catalytic activity for oxidative desulfurization. *Fuel* **2014**, *117*, 667–673. [CrossRef]
10. Shao, B.B.; Shi, L.; Meng, X. Deep desulfurization of 4,6-dimethyldienzothiophene by an ionic liquids extraction coupled with catalytic oxidation with a molybdic compound. *Ind. Eng. Chem. Res.* **2014**, *53*, 6655–6663. [CrossRef]
11. Wang, D.H.; Liu, N.; Zhang, J.Y.; Zhao, X.; Zhang, W.H.; Zhang, M.H. Oxidative desulfurization using ordered mesoporous silicas as catalysts. *J. Mol. Catal. A Chem.* **2014**, *393*, 47–55. [CrossRef]

12. Zhang, M.; Zhu, W.S.; Li, H.P.; Xun, S.H.; Li, M.; Li, Y.N.; Wei, Y.C.; Li, H.M. Fabrication and characterization of tungsten-containing mesoporous silica for heterogeneous oxidative desulfurization. *Chin. J. Catal.* **2016**, *37*, 971–978. [CrossRef]
13. Zhu, W.S.; Gu, Q.Q.; Hu, J.J.; Wu, P.W.; Yin, S.; Zhu, F.X.; Zhang, M.; Xiong, J.; Li, H.M. Fabrication of functional dual-mesoporous silicas by using peroxo-tungstate ionic liquid and their applications in oxidative desulfurization. *J. Porous Mater.* **2015**, *22*, 1227–1233. [CrossRef]
14. Li, Y.N.; Zhang, M.; Zhu, W.S.; Li, M.; Xiong, J.; Zhang, Q.; Wei, Y.C.; Li, H.M. One-pot synthesis and characterization of tungsten-containing meso-ceria with enhanced heterogenous oxidative desulfurization in fuels. *RSC Adv.* **2016**, *6*, 68922–68928. [CrossRef]
15. Collins, T.J. Designing ligands for oxidizing complexes. *Acc. Chem. Res.* **1994**, *27*, 279–285. [CrossRef]
16. Bianchini, C.; Jimenez, M.V.; Meli, A.; Moneti, S.; Vizza, F.; Herrera, V.; Sanchezdelgado, R.A. Hydrodesulfurization (HDS) model systems. Opening, hydrogenation, and hydrodesulfurization of dibenzothiophene (DBT) at iridium. First case of catalytic HDS of DBT in homogeneous phase. *Organometallics* **1995**, *14*, 2342–2352. [CrossRef]
17. And, D.A.V.; Jones, W.D. Hydrodesulfurization of thiophene and benzothiophene to butane and ethylbenzene by a homogeneous Iridium Complex. *Organometallics* **1997**, *16*, 1912–1919.
18. Li, H.; And, G.B.C.; Sweigart, D.A. Models for homogeneous deep hydrodesulfurization. Intramolecular CO substitution by the sulfur in $[(\eta^6$-2-methylbenzothiophene$)Mn(CO)_3]^+$ and $[(\eta^6$-dibenzothiophene$)Mn(CO)_3]^+$ after regiospecific insertion of platinum into a C−S Bond. *Organometallics* **2000**, *19*, 1823–1825. [CrossRef]
19. Hasan, Z.; Jeon, J.; Jhung, S.H. Oxidative desulfurization of benzothiophene and thiophene with WO_x/ZrO_2 catalysts: Effect of calcination temperature of catalysts. *J. Hazard. Mater.* **2012**, *205*, 216–221. [CrossRef]
20. Wan, A.W.A.B.; Ali, R.; Kadir, A.A.A.; Wan, N.A.W.M. Effect of transition metal oxides catalysts on oxidative desulfurization of model diesel. *Fuel Process. Technol.* **2012**, *101*, 78–84.
21. Chen, X.; Zhang, J.; Fu, X.; Antonietti, M.; Wang, X. Fe-g-C_3N_4-catalyzed oxidation of benzene to phenol using hydrogen peroxide and visible light. *J. Am. Chem. Soc.* **2009**, *131*, 11658–11659. [CrossRef]
22. Haw, K.G.; Wan, A.W.A.B.; Ali, R.; Chong, J.F.; Kadir, A.A.A. Catalytic oxidative desulfurization of diesel utilizing hydrogen peroxide and functionalized-activated carbon in a biphasic diesel–acetonitrile system. *Fuel Process. Technol.* **2010**, *91*, 1105–1112. [CrossRef]
23. Li, X.; Huang, S.; Xu, Q.; Yang, Y. Preparation of WO_3-SBA-15 mesoporous molecular sieve and its performance as an oxidative desulfurization catalyst. *Transit. Met. Chem.* **2009**, *34*, 943. [CrossRef]
24. And, Y.W.C.; Lu, Y.H. Characteristics of V-MCM-41 and its catalytic properties in oxidation of benzene. *Ind. Eng. Chem. Res.* **1999**, *38*, 1893–1903.
25. Lü, H.; Gao, J.; Jiang, Z.; Yang, Y.; Song, B.; Li, C. Oxidative desulfurization of dibenzothiophene with molecular oxygen using emulsion catalysis. *Chem. Commun.* **2006**, *2*, 150–152. [CrossRef] [PubMed]
26. Craven, M.; Xiao, D.; Kunstmann-Olsen, C.; Kozhevnikova, E.F.; Blanc, F.; Steiner, A.; Kozhevnikov, I.V. Oxidative desulfurization of diesel fuel catalyzed by polyoxometalate immobilized on phosphazene-functionalized silica. *Appl. Catal. B Environ.* **2018**, *231*, 82–91. [CrossRef]
27. Zhang, X.M.; Zhang, Z.H.; Zhang, B.H.; Yang, X.F.; Chang, X.; Zhou, Z.; Wang, D.H.; Zhang, M.H.; Bu, X.H. Synergistic effect of Zr-MOF on phosphomolybdic acid promotes efficient oxidative desulfurization. *Appl. Catal. B Environ.* **2019**, *256*, 117804. [CrossRef]
28. Li, C.; Jiang, Z.X.; Gao, J.B.; Yang, Y.X.; Wang, S.J.; Tian, F.P.; Sun, F.X.; Sun, X.P.; Ying, P.L.; Han, C.R. Ultra-deep desulfurization of diesel: Oxidation with a recoverable catalyst assembled in emulsion. *Chem. Eur. J.* **2004**, *10*, 2277–2280. [CrossRef]
29. Lu, H.Y.; Gao, J.B.; Jiang, Z.X.; Jing, F.; Yang, Y.X.; Wang, G.; Li, C. Ultra-deep desulfurization of diesel by selective oxidation with $[C_{18}H_{37}N(CH_3)_3]_4[H_2NaPW_{10}O_{36}]$ catalyst assembled in emulsion droplets. *J. Catal.* **2006**, *239*, 369–375. [CrossRef]
30. Qiu, J.; Wang, G.; Zhang, Y.; Zeng, D.; Yang, C. Direct synthesis of mesoporous $H_3PMo_{12}O_{40}/SiO_2$ and its catalytic performance in oxidative desulfurization of fuel oil. *Fuel* **2015**, *147*, 195–202. [CrossRef]
31. Li, Y.Q.; Qu, J.Y.; Gao, F.; Lv, S.Y.; Shi, L.; He, C.X.; Sun, J.C. In situ fabrication of Mn_3O_4 decorated graphene oxide as a synergistic catalyst for degradation of methylene blue. *Appl. Catal. B Environ.* **2015**, *162*, 268–274. [CrossRef]
32. Mamlouk, M.; Ocon, P.; Scott, K. Preparation and characterization of polybenzimidzaole/diethylamine hydrogen sulphate for medium temperature proton exchange membrane fuel cells. *J. Power Sour.* **2014**, *245*, 915–926. [CrossRef]
33. Kohno, Y.; Haga, E.; Yoda, K.; Shibata, M.; Fukuhara, C.; Tomita, Y.; Maeda, Y.; Kobayashi, K. Adsorption behavior of natural anthocyanin dye on mesoporous silica. *J. Phys. Chem. Solids* **2014**, *75*, 48–51. [CrossRef]
34. Szot, K.; Niedziolka, J.; Rogalski, J.; Marken, F.; Opallo, M. Bioelectrocatalytic dioxygen reduction at hybrid silicate-polyallylamine film with encapsulated laccase. *J. Electroanal. Chem.* **2008**, *612*, 1–8. [CrossRef]
35. Latonen, R.M.; Esteban, B.M.; Kvarnstrom, C.; Ivaska, A. Electrochemical polymerization and characterization of a poly(azulene)-TiO_2 nanoparticle composite film. *J. Appl. Electrochem.* **2009**, *39*, 653–661. [CrossRef]
36. Xie, G.Q.; Xi, P.X.; Liu, H.Y.; Chen, F.J.; Huang, L.; Shi, Y.J.; Hou, F.P.; Zeng, Z.Z.; Shao, C.W.; Wang, J. A facile chemical method to produce superparamagnetic graphene oxide-Fe_3O_4 hybrid composite and its application in the removal of dyes from aqueous solution. *J. Mater. Chem.* **2012**, *22*, 1033–1039. [CrossRef]

37. Sun, X.W.; Liu, S.M.; Zhang, S.; Dang, T.Y.; Tian, H.R.; Lu, Y.; Liu, S.X. High proton conductivity achieved by the self-assembly of POM-based acid-base adduct in SBA-15 over a wide range from −40 to 85 °C. *ACS Appl. Energy. Mater.* **2020**, *3*, 1242–1248. [CrossRef]
38. Yuan, J.J.; Xiong, J.; Wang, J.H.; Ding, W.J.; Yang, L.; Zhang, M.; Zhu, W.S.; Li, H.M. Structure and catalytic oxidative desulfurization properties of SBA-15 supported silicotungstic acid ionic liquid. *J. Porous Mater.* **2016**, *23*, 823–831. [CrossRef]
39. Xun, S.H.; Zhu, W.S.; Zhu, F.X.; Chang, Y.H.; Zheng, D.; Qin, Y.J.; Zhang, M.; Jiang, W.; Li, H.M. Design and synthesis of W-containing mesoporous material with excellent catalytic activity for the oxidation of 4,6-DMDBT in fuels. *Chem. Eng. J.* **2015**, *280*, 256–264. [CrossRef]
40. Zhang, M.; Zhu, W.S.; Xun, S.H.; Xiong, J.; Ding, W.J.; Li, M.; Wang, Q.; Li, H.M. Enhanced Oxidative desulfurization of dibenzothiophene by functional Mo-containing mesoporous silica. *Chem. Eng. Technol.* **2015**, *38*, 117–124. [CrossRef]
41. Guo, T.; Jiang, W.; Ruan, Y.J.; Dong, L.; Liu, H.; Li, H.P.; Zhu, W.S.; Li, H.M. Superparamagnetic Mo-containing core-shell microspheres for catalytic oxidative desulfurization of fuel. *Colloids Surf. A* **2018**, *537*, 243–249. [CrossRef]
42. Zhang, M.; Zhu, W.S.; Li, H.P.; Li, M.; Yin, S.; Li, Y.N.; Wei, Y.C.; Li, H.M. Facile fabrication of molybdenum-containing ordered mesoporous silica induced deep desulfurization in fuel. *Colloids Surf. A* **2016**, *504*, 174–181. [CrossRef]
43. Zhang, X.; Li, H.M.; Wan, H.L.; Weng, W.Z.; Yi, X.D. Studies on VPO/SiO_2 catalyst for selective oxidation of propane. *Chin. J. Catal.* **2003**, *24*, 87–92.
44. Fang, Z.H.; Yang, D.G.; Gao, Y.; Li, H.M. Massage ball-like, hollow porous Au/SiO_2 microspheres templated by a Pickering emulsion derived from poylmer-metal hybrid emulsifier micelles. *RSC Adv.* **2014**, *4*, 49866–49872. [CrossRef]
45. Xu, X.Y.; Liu, Y.J.; Gao, Y.; Li, H.M. Preparation of Au@silica Janus nanosheets and their catalytic application. *Colloids Surf. A* **2017**, *529*, 613–620. [CrossRef]
46. Zhang, F.; Braun, G.B.; Pallaoro, A.; Zhang, Y.C.; Shi, Y.F.; Cui, D.X.; Moskovits, M.; Zhao, D.Y.; Stucky, G.D. Mesoporous multifunctional upconversion luminescent and magnetic "nanorattle" materials for targeted chemotherapy. *Nano Lett.* **2012**, *12*, 61–67. [CrossRef]
47. Xu, C.; De, S.; Balu, A.M.; Ojeda, M.; Luque, R. Mechanochemical synthesis of advanced nanomaterials for catalytic applications. *Chem. Commun.* **2015**, *46*, 6698–6713. [CrossRef]
48. Ralphs, K.; Hardacre, C.; James, S.L. Application of heterogeneous catalysts prepared by mechanochemical synthesis. *Chem. Soc. Rev.* **2013**, *42*, 7701–7718. [CrossRef] [PubMed]
49. Seo, P.W.; Lee, J.Y.; Shim, K.S.; Hong, S.H.; Hong, S.C.; Hong, S.I. The control of valence state: How V/TiO_2 catalyst is hindering the deactivation using the mechanochemical method. *J. Hazard. Mater.* **2009**, *165*, 39–47. [CrossRef] [PubMed]
50. Yan, X.M.; Mei, P.; Lei, J.; Mi, Y.; Xiong, L.; Guo, L. Synthesis and characterization of mesoporous phosphotungstic acid/TiO_2 nanocomposite as a novel oxidative desulfurization catalyst. *J. Mol. Catal. A Chem.* **2009**, *304*, 52–57. [CrossRef]
51. Eimer, G.A.; Casuscelli, S.G.; Ghione, G.E.; Crivello, M.E.; Herrero, E.R. Synthesis, characterization and selective oxidation properties of Ti-containing mesoporous catalysts. *Appl. Catal. A Gen.* **2006**, *298*, 232–242. [CrossRef]
52. Zhang, M.; Zhu, W.; Xun, S.; Li, H.; Gu, Q.; Zhao, Z.; Wang, Q. Deep oxidative desulfurization of dibenzothiophene with POM-based hybrid materials in ionic liquids. *Chem. Eng. J.* **2013**, *220*, 328–336. [CrossRef]
53. Yu, Y.; Wu, Q.; Guo, Y.; Hu, C.; Wang, E. Efficient degradation of dye pollutants on nanoporous polyoxotungstate–anatase composite under visible-light irradiation. *J. Mol. Catal. A Chem.* **2005**, *225*, 203–212.
54. Arellano, U.; Wang, J.A.; Timko, M.T.; Chen, L.F.; Carrera, S.P.P.; Asomoza, M.; Vargas, O.A.G.; Llanos, M.E. Oxidative removal of dibenzothiophene in a biphasic system using sol–gel $FeTiO_2$ catalysts and H_2O_2 promoted with acetic acid. *Fuel* **2014**, *126*, 16–25. [CrossRef]
55. Yuan, Z.Y.; Zhang, X.B.; Su, B.L. Moderate hydrothermal synthesis of potassium titanate nanowires. *Appl. Phys. A* **2004**, *78*, 1063–1066. [CrossRef]
56. And, C.K.; Trakarnpruk, W. Oxidative desulfurization using polyoxometalates. *Ind. Eng. Chem. Res.* **2006**, *45*, 1853–1856.
57. Li, H.P.; Zhu, W.S.; Zhu, S.W.; Xia, J.X.; Chang, Y.H.; Jiang, W.; Zhang, M.; Zhou, Y.W.; Li, H.M. The Selectivity for sulfur removal from oils: An insight from conceptual density functional theory. *AIChE J.* **2016**, *62*, 2087–2100. [CrossRef]
58. Li, M.; Zhang, M.; Wei, A.M.; Zhu, W.S.; Xun, S.H.; Li, Y.A.; Li, H.P.; Li, H.M. Facile synthesis of amphiphilic polyoxometalate-based ionic liquid supported silica induced efficient performance in oxidative desulfurization. *J. Mol. Catal. A Chem.* **2015**, *406*, 23–30. [CrossRef]